Multidiscipline Modeling in Materials and Structures

Unsteady natural convection flow of a rotating fluid past an exponential accelerated vertical plate with Hall current, ion-slip and magnetic effect

Jitendra Kumar Singh, Srinivasa C.T.,

The current issue and full text archive of this journal is available on Emerald Insight at:
www.emeraldinsight.com/1573-6105.htm

Received 7 June 2017
Revised 6 August 2017
Accepted 31 October 2017

Unsteady natural convection flow of a rotating fluid past an exponential accelerated vertical plate with Hall current, ion-slip and magnetic effect

Jitendra Kumar Singh
Department of Mathematics, Vijayanagara Sri Krishnadevaraya University, Ballari, India, and
Srinivasa C.T.
Department of Mathematics, Vedavathi Government First Grade College, Hiriyur, India

Abstract

Purpose – The purpose of this paper is to deal with an unsteady natural convection flow of a rotating fluid past an exponential accelerated vertical plate. The effect of Hall current, ion-slip and magnetic field is considered. Two types of plate temperature, namely, uniform and ramped temperature are considered to model heat transfer analysis.

Design/methodology/approach – The Laplace transform technique is employed to find the closed form solutions for velocity, temperature and concentration.

Findings – The effects of flow governing parameters on the velocity profile, temperature profile, concentration profile, skin friction, Nusselt and Sherwood numbers are discussed and presented through graphs and tables. It is found that fluid velocity in the primary flow direction decreases with the increase in the magnetic parameter.

Originality/value – First time in the literature, the authors obtained closed form solution to natural convection flow of a rotating fluid past an exponential accelerated vertical plate.

Keywords Permeability, Natural convection, rotation, Hall current, Ion-slip

Paper type Research paper

Nomenclature

B_0	applied magnetic field (T)
C	dimensionless species concentration
C'	species concentration (mol/m^3)
C'_w	a constant concentration (mol/m^3)
C'_∞	free stream concentration (mol/m^3)
C_p	specific heat at constant pressure (J/kg.K)
D	chemical molecular diffusivity (m^2/s)
K	rotation parameter
g	acceleration due to gravity (m/s^2)
G_C	solutal Grashof number
G_T	thermal Grashof number
k	thermal conductivity of the fluid (W/m.K)
k'	permeability (m^2)
k_1	permeability parameter
K'	chemical reaction constant
K_1	chemical reaction parameter
M	magnetic parameter
P_r	Prandtl number
Q_0	heat absorption coefficient (W/m^2.K)
S_c	Schmdit number
t	dimensionless time
t'	time (s)
T'	fluid temperature (K)
T'_w	a constant temperature (K)
T'_∞	free stream temperature (K)
u	dimensionless velocity in x-direction
w	dimensionless velocity in z-direction
y	dimensionless coordinate normal to the plate

Multidiscipline Modeling in Materials and Structures
Vol. 14 No. 2, 2018
pp. 216-235

1573-6105
DOI 10.1108/MMMS-06-2017-0045

β_C volumetric coefficient of species concentration expansion
β_e Hall parameter
β_i ion-slip parameter
β_T volumetric coefficient of thermal expansion (K^{-1})
υ kinematic viscosity (m^2/s)
ϕ heat source parameter
ρ fluid density (kg/m^3)
σ electrical conductivity (S/m)
τ_x dimensionless skin friction component in x-direction
τ_z dimensionless skin friction component in z-direction
θ non-dimensional fluid temperature

1. Introduction

The study of unsteady natural convection heat and mass transfers flow of an electrically conducting fluid over a vertical plate has wide range of applications in various engineering as well as in the industrial fields such as heat exchange devices, geophysics, astrophysics, thermal insulators, electronic equipment cooling processes, etc. By considering its applications, many researchers have shown their keen interest in this field. Das *et al.* (2014) discussed an unsteady free convection flow over a vertical plate in the presence of ramped wall temperature and radiation effect. Hossain *et al.* (2015) employed explicit finite difference method to investigate the time dependent free convection flow of a fluid in the presence of viscosity effect. An analysis has been carried out on unsteady free convection flow by Foisal and Alam (2016) over an inclined plane in the presence of magnetic field. Tkachenko *et al.* (2016) utilized both numerical and experimental method to study the time dependent natural convection fluid flow in an open ended channel. Zargartalebi *et al.* (2017) considered time periodic boundary conditions in the analysis of unsteady natural convection flow in a porous cavity. A scaling analysis was carried out by Lin and Armfield (2017) to study an unsteady natural convection boundary layer flow of a Newtonian fluid and they recognized the three heating stages called start-up, a transitional and a quasi-steady stage.

The concept of fluid flow, heat and mass transfers with rotating environment plays a very dominant role in the applications of geophysics, petrochemical engineering, meteorology, oceanography and aeronautics. The stimulus for scientific research on rotating fluid system is basically originated from geophysical and fluid engineering applications. Many aspects of the motion of terrestrial and planetary atmospheres are highly influenced by the effect of rotation. Rotation flow theory is utilized in determining the viscosity of the fluid, in the construction of the turbine and other centrifugal machines. Greenspan and Howard (1963) have considered the closed axisymmetric container which is filled with viscous fluid to describe the unsteady rotating flow behavior. Nazar *et al.* (2004) have derived perturbation and asymptotic solutions for smaller and larger time, respectively, in an unsteady flow problem of rotating fluid. Sarma and Pandit (2016) obtained an exact solution using analytical method called the Laplace transform technique in the free convection heat and mass transfers of a Newtonian fluid flow problem with the rotation effect. The influence of rotational system on nanofluid flow was explored by Mustafa *et al.* (2017) and they have found that the effect of rotational parameter reduces the heat transfer coefficient. Mohamad *et al.* (2017) have considered the non-coaxial rotation of an oscillating vertical disk to describe the heat and mass transfers of viscous fluid.

The effect of Hall current and ion-slip plays a remarkable role in various applications such as power generators, MHD accelerators, refrigeration coils, transmission lines, electric transformers, heating elements, etc. These effects are applied when the strong magnetic field is taken into consideration. In this case, diffusion velocity of ions should be considered. Singh, Joshi, Begum and Srinivasa (2016) have examined the influence of Hall current in an unsteady heat and mass transfers flow of viscous rotating fluid. Further, they have studied the natural convection, thermal and mass diffusions process. Hayat *et al.* (2016) addressed the impact of Hall and ion-slip in the mixed convective flow of non-Newtonian nanofluid. Singh, Begum and Joshi (2016) have discussed the unsteady Couette flow of MHD viscous fluid in the rotating system in the presence of Hall current and ion-slip effect. The significance of Hall and ion-slip parameter on mixed convection flow of nanofluid has been analyzed by Srinivasacharya and Shafeeurrahaman (2017).

Various physical processes such as convection in Earth's mantle, modeling of fire and combustion, development of metal waste from spent nuclear fuel, post-accident heat removal, fluids undergoing exothermic and/or endothermic chemical reaction, etc. exhibit the consequential role of heat generation on heat transfer characteristics of hydromagnetic free convective flows. Further, the influence of chemical reaction on unsteady hydromagnetic free convective flow with heat and mass transfers has been a subject of great attention in the last few decades. The research initiative in this field has enlarged because of wide range of applications in different areas of science and technology. The effects of Hall current, ion-slip current and heat generation are discussed by Ram (1995) in the free convective rotating fluid flow. Comparison of fluid flow over an isothermal plate and ramped temperature plate was made by Seth and Sarkar (2015) in the presence of chemical reaction and heat generation effect. Gireesha *et al.* (2016) have considered two temperature boundary conditions, i.e. PHF and PST case to study the heat source/sink effect for the boundary layer flow of stretching surface. Krishnamurthy *et al.* (2016) have considered the chemical reaction effect while studying the boundary layer flow of Williamson fluid with suspended nanoparticles. Combined effect of Hall current and rotation system for time dependent heat and mass transfer flow of viscous fluid was formulated by Hussain *et al.* (2017).

In the view of aforementioned applications, we intended to analyze an unsteady natural convection flow of a rotating fluid past an exponential accelerated vertical plate with Hall current, ion-slip and magnetic effect. The exact solution for velocity, temperature and concentration is obtained using the Laplace transform technique. The effects of several dimensionless parameters on the velocity, temperature, concentration profiles, skin friction, Nusselt and Sherwood numbers have been discussed through graphical and tabular representations in detail.

2. Mathematical model of the problem

Consider an unsteady hydromagnetic heat and mass transfers flow of an incompressible, viscous, electrically conducting, heat absorbing and chemically reacting fluid past a vertical plate in presence of Hall current and ion-slip, embedded in a uniform porous medium. The Cartesian coordinate system (x', y', z') is considered as frame of reference. The x'-axis is chosen in such a way that it is along the plate in upward direction, y'-axis is normal to the plane of the plate and z'-axis is perpendicular to $x'y'$-plane. Flow past vertical plate is permeated by a uniform transverse magnetic field B_0 applied along y'-direction. The fluid and the plate rotate unison as rigid body with uniform angular velocity $\overrightarrow{\Omega}$ about y'-axis. It is assumed that initially, the fluid and plate are at rest. The temperature and species concentration at the plate are assumed to be T'_∞ and C'_∞, respectively. Suddenly, at time $t' > 0$, the plate is assumed to be exponentially accelerated with velocity $U_0 e^{U_0^2 t'/\upsilon}$ in the vertical upward direction. At the same time, the species concentration near the plate raised linearly with time t' to $C'_\infty + (C'_w - C'_\infty)U_0^2 t'/\upsilon$. We have considered two particular cases for plate temperature:

(1) Uniform plate temperature: at time $t' > 0$, the plate temperature is raised to T'_w.

(2) Ramped plate temperature: at time $t' > 0$, the plate temperature is raised linearly with time t' to $T'_\infty + (T'_w - T'_\infty)U_0^2 t'/\upsilon$ when $0 < t' \leqslant \upsilon/U_0^2$ and thereafter it is maintained at uniform temperature T'_w when $t' > \upsilon/U_0^2$.

Since the plate is electrically non-conducting and is of infinite extent along x' and z'-directions, so all physical quantities will be function of y' and t' only. The physical model of the problem is presented in Figure 1.

The fluid considered is emitting/absorbing radiation but non-scattering. It is also assumed that the diffusion species and fluid particles. There is no applied or polarization voltages imposed on the flow-field so the electric field $\overrightarrow{E}$ is assumed to be 0 v $\overrightarrow{E}' = (0, 0, 0)$ (Meyer, 1958). The induced magnetic field generated by fluid motion is assumed to be negligible in comparison to applied one because fluid is assumed to be partially ionized and the magnetic Reynold's number $R_m \ll 1$ (Cramer and Pai, 1973).

In the essence of above made assumptions, the governing equations for an unsteady hydromagnetic flow heat and mass transfers natural convection flow past an exponentially accelerated vertical plate in a porous medium in the presence of thermal and mass diffusions with Hall current, ion-slip and rotation under usual Boussinesq's approximation are given by:

$$\frac{\partial \overrightarrow{q}'}{\partial t'} + 2\vec{\Omega} \times \overrightarrow{q}' = \upsilon \nabla^2 \overrightarrow{q}' + \frac{1}{\rho}\left(\overrightarrow{J}' \times \overrightarrow{B}'\right) + \overrightarrow{g}\beta_T\left(T' - T'_\infty\right)$$

$$+ \overrightarrow{g}\beta_C\left(C' - C'_\infty\right) - \frac{\upsilon \overrightarrow{q}'}{k'}. \tag{1}$$

The energy equation with thermal diffusion is represented as follows:

$$\frac{\partial T'}{\partial t'} = \frac{k}{\rho C_p}\frac{\partial^2 T'}{\partial y'^2} - \frac{Q_0\left(T' - T'_\infty\right)}{\rho C_p}. \tag{2}$$

The concentration equation with chemical molecular diffusion is given by:

$$\frac{\partial C'}{\partial t'} = D\frac{\partial^2 C'}{\partial y'^2} - K'\left(C' - C'_\infty\right). \tag{3}$$

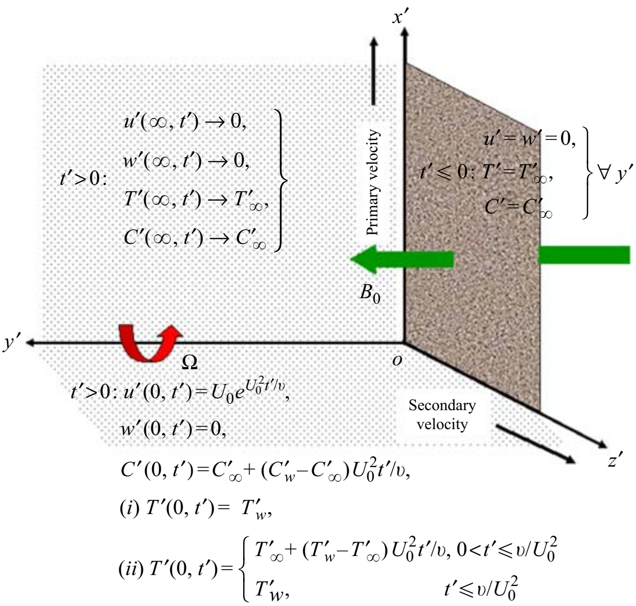

Figure 1.
Physical model of the problem

Ohm's law for a moving conductor taking Hall and ion-slip currents into account is represented as (Sutton and Sherman, 1965):

$$\vec{J}' = \sigma\left[\vec{E}' + \left(\vec{q}' \times \vec{B}'\right)\right] - \frac{\beta_e}{B_0}\left(\vec{J}' \times \vec{B}'\right) + \frac{\beta_e\beta_i}{{B_0}^2}\left(\vec{J}' \times \vec{B}'\right) \times \vec{B}'. \tag{4}$$

Using Equation (4) in Equation (1), the equation of motion for MHD free convective flow of an incompressible, chemically reacting, electrically and thermally conducting fluid past a vertical plate embedded in a porous medium in a rotating system taking Hall and ion-slip currents into account, in component form, become:

$$\frac{\partial u'}{\partial t'} + 2\Omega w' = \upsilon\frac{\partial^2 u'}{\partial y'^2} - \frac{\sigma B_0^2}{\rho}\frac{(u'\alpha_e + w'\beta_e)}{(\alpha_e^2 + \beta_e^2)} + g\beta_T(T' - T'_\infty) + g\beta_C(C' - C'_\infty) - \frac{\upsilon u'}{k'}, \tag{5}$$

$$\frac{\partial w'}{\partial t'} + 2\Omega u' = \upsilon\frac{\partial^2 w'}{\partial y'^2} - \frac{\sigma B_0^2}{\rho}\frac{(w'\alpha_e - u'\beta_e)}{(\alpha_e^2 + \beta_e^2)} - \frac{\upsilon w'}{k'}, \tag{6}$$

where $\alpha_e = 1 + \beta_e\beta_i$.

The initial and boundary conditions correspond to the two particular cases of fluid flows are given below.

For uniform plate temperature:

$$t' \leqslant 0 : u' = w' = 0,\ T' = T'_\infty,\ C' = C'_\infty \quad \forall y', \tag{7}$$

$$\left.\begin{aligned} & t' > 0 : u' = U_0 e^{U_0^2 t'/\upsilon},\ w' = 0,\ T' = T'_w, \\ & C' = C'_\infty + (C'_w - C'_\infty)U_0^2 t'/\upsilon \quad \text{at} \quad y' = 0; \\ & u' \to 0,\ w' \to 0,\ T' \to T'_\infty,\ C' \to C'_\infty \quad \text{as} \quad y' \to \infty. \end{aligned}\right\} \tag{8}$$

For ramped plate temperature:

$$t' \leqslant 0 : u' = w' = 0,\ T' = T'_\infty,\ C' = C'_\infty \quad \forall y', \tag{9}$$

$$\left.\begin{aligned} & t' > 0 : u' = U_0 e^{U_0^2 t'/\upsilon},\ w' = 0, \\ & C' = C'_\infty + (C'_w - C'_\infty)U_0^2 t'/\upsilon, \\ & T' = \begin{cases} T'_\infty + (T'_w - T'_\infty)U_0^2 t'/\upsilon \\ \text{when } 0 < t' \leqslant \upsilon/U_0^2, \qquad \text{at } y' = 0; \\ T'_w \quad \text{when } t' > \upsilon/U_0^2, \end{cases} \\ & u' \to 0,\ w' \to 0, \quad T' \to T'_\infty, \quad C' \to C'_\infty \text{ as } y' \to \infty. \end{aligned}\right\} \tag{10}$$

We now define the following non-dimensional quantities:

$$y = y'U_0/\upsilon,\ u = u'/U_0,\ w = w'/U_0,\ \theta = (T' - T'_\infty)/(T'_w - T'_\infty),$$
$$C = (C' - C'_\infty)/(C'_w - C'_\infty).$$

Using above defined non-dimensional quantities and $F = u + iw$ in Equations (2) and (3) and (5) and (6), one can get:

$$\frac{\partial F}{\partial t} - 2iK^2F = \frac{\partial^2 F}{\partial y^2} - \frac{M^2F}{\alpha_e^2 + \beta_e^2}(\alpha_e - i\beta_e) + G_T\theta + G_C C - \frac{F}{k_1}, \tag{11}$$

$$\frac{\partial \theta}{\partial t} = \frac{1}{P_r}\frac{\partial^2 \theta}{\partial y^2} - \phi\theta, \tag{12}$$

$$\frac{\partial C}{\partial t} = \frac{1}{S_c}\frac{\partial^2 C}{\partial y^2} - K_1 C, \tag{13}$$

where $K^2 = \Omega\upsilon/U_0^2$, $M^2 = \sigma B_0^2\upsilon/\rho U_0^2$, $G_T = \upsilon g\beta'_T(T'_w - T'_\infty)/U_0^3$, $G_C = \upsilon g\beta'_C(C'_w - C'_\infty)/U_0^3$, $k_1 = k' U_0^2/\upsilon^2$, $P_r = \rho C_p\upsilon/k$, $\phi = Q_0\upsilon/\rho C_p U_0^2$, $S_c = \upsilon/D$ and $K_1 = K'\upsilon/U_0^2$.

The non-dimensional initial and boundary conditions for fluid flow are given below.

For uniform plate temperature:

$$t \leqslant 0: F = 0,\ \ \theta = 0,\ \ C = 0 \quad \forall y, \tag{14}$$

$$\left.\begin{array}{l} t > 0: F = e^t,\ \theta = 1,\ C = t \quad \text{at } y = 0; \\ F \to 0,\ \theta \to 0,\ C \to 0 \quad \text{as } y \to \infty. \end{array}\right\} \tag{15}$$

For ramped plate temperature:

$$t \leqslant 0: F = 0,\ \theta = 0,\ C = 0 \quad \forall y, \tag{16}$$

$$\left.\begin{array}{l} t > 0: F = e^t,\ C = t,\ \theta = \begin{cases} t & \text{when } 0 < t \leqslant 1, \\ 1 & \text{when } t > 1 \end{cases} \quad \text{at } y = 0; \\ F \to 0,\ \theta \to 0,\ C \to 0 \quad \text{as } y \to \infty. \end{array}\right\} \tag{17}$$

3. Solution of the problem

Now we shall find the analytical solution of governing Equations (11)-(13) subject to the initial and boundary conditions (14)-(15) and (16)-(17) using the Laplace transform method.

Laplace transform of Equations (11)-(13) and using initial condition (14)/(16), one can obtain:

$$\frac{d^2\overline{F}}{dy^2} - \left[s + \frac{1}{k_1} + \frac{M^2\alpha_e}{\alpha_e^2 + \beta_e^2} - i\left(2K^2 + \frac{\beta_e M^2}{\alpha_e^2 + \beta_e^2}\right)\right]\overline{F} + G_T\overline{\theta} + G_C\overline{C} = 0, \tag{18}$$

$$\frac{d^2\overline{\theta}}{dy^2} - P_r(s + \phi)\overline{\theta} = 0, \tag{19}$$

$$\frac{d^2\overline{C}}{dy^2} - S_c(s + K_1)\overline{C} = 0, \tag{20}$$

where $\overline{F}(y,s) = \int_0^\infty e^{-st}F(y,t)dt$, $\overline{\theta}(y,s) = \int_0^\infty e^{-st}\theta(y,t)dt$, $\overline{C}(y,s) = \int_0^\infty e^{-st}C(y,t)dt$, and s (>0) is Laplace parameter.

The boundary conditions (15) and (17) after taking Laplace transform assume the following form.

For uniform plate temperature:

$$\left.\begin{aligned}&\overline{F}=\tfrac{1}{s-1},\ \overline{\theta}=\tfrac{1}{s},\ \overline{C}=\tfrac{1}{s^2}\quad \text{at } y=0;\\ &\overline{F}\to 0,\ \overline{\theta}\to 0,\ \overline{C}\to 0\quad \text{as } y\to\infty.\end{aligned}\right\} \tag{21}$$

For ramped plate temperature:

$$\left.\begin{aligned}&\overline{F}=\tfrac{1}{s-1},\ \overline{\theta}=\tfrac{1}{s^2}(1-e^{-s}),\ \overline{C}=\tfrac{1}{s^2}\quad \text{at } y=0;\\ &\overline{F}\to 0,\ \overline{\theta}\to 0,\ \overline{C}\to 0\quad \text{as } y\to\infty.\end{aligned}\right\} \tag{22}$$

Solving Equations (18)-(20) subject to the boundary conditions (21) and (22) and then inverting, the solution for fluid velocity, temperature and species concentration is obtained, and is represented by the following.

For uniform plate temperature:

$$\begin{aligned}F(y,t)=F_1(y,t,1,m_3,1)&+\frac{G_T}{X_1(P_r-1)}\{F_1(y,t,1,m_3,0)-F_1(y,t,P_r,\phi,0)\\ &-F_1(y,t,1,m_3,-X_1)-F_1(y,t,P_r,\phi,-X_1)\}-\frac{G_C}{X_2^2(S_c-1)}\{F_1(y,t,1,m_3,0)\\ &-F_1(y,t,S_c,K_1,0)-F_1(y,t,1,m_3,-X_2)+F_1(y,t,S_c,K_1,-X_2)\\ &-X_2\{F_2(y,t,1,m_3,0)-F_2(y,t,S_c,K_1,0)\}\},\end{aligned} \tag{23}$$

$$\theta(y,\ t)=F_1(y,\ t,\ P_r,\ \phi,\ 0), \tag{24}$$

$$C(y,\ t)=F_2(y,\ t,\ S_c,\ K_1,\ 0). \tag{25}$$

For ramped plate temperature:

$$\begin{aligned}F(y,t)=F_1(y,t,1,m_3,1)&+\frac{G_T}{(P_r-1)}\frac{1}{X_1^2}[\{X_1(F_2(y,t,1,m_3,0)-F_2(y,t,P_r,\phi,0))\\ &-(F_1(y,t,1,m_3,0)-F_1(y,t,P_r,\phi,0)-F_1(y,t,1,m_3,-X_1)\\ &+F_1(y,t,P_r,\phi,-X_1))\}-H(t-1)\{X_1(F_2(y,t-1,1,m_3,0)\\ &-F_2(y,t-1,P_r,\phi,0))-(F_1(y,t-1,1,m_3,0)-F_1(y,t-1,P_r,\phi,0)\\ &-F_1(y,t-1,1,m_3,-X_1)+F_1(y,t-1,P_r,\phi,-X_1))\}]\\ &+\frac{G_C}{(S_c-1)X_2^2}[X_2(F_2(y,t,1,m_3,0)-F_2(y,t,S_c,K_1,0))-(F_1(y,t,1,m_3,0)\\ &-F_1(y,t,S_c,K_1,0)-F_1(y,t,1,m_3,-X_2)+F_1(y,t,S_c,K_1,-X_2))],\end{aligned} \tag{26}$$

$$\theta(y,\ t)=F_2(y,\ t,\ P_r,\ \phi,\ 0)-H(t-1)F_2(y,\ t-1,\ P_r,\ \phi,\ 0), \tag{27}$$

$$C(y,\ t)=F_2(y,\ t,\ S_c,\ K_1,\ 0), \tag{28}$$

where:

$$X_1=\frac{1}{P_r-1}(P_r\phi-m_3),\ \ X_2=\frac{1}{S_c-1}(S_cK_1-m_3),$$

$$m_3=\frac{1}{k_1}+\frac{M^2\alpha_e}{\alpha_e^2+\beta_e^2}-i\left(2K^2+\frac{\beta_e M^2}{\alpha_e^2+\beta_e^2}\right),$$

$$F_1(y,t,a,b,c)=\frac{e^{ct}}{2}\left[e^{y\sqrt{a}\sqrt{b+c}}erfc\left(\frac{y}{2}\sqrt{\frac{a}{t}}+\sqrt{(b+c)t}\right)+e^{-y\sqrt{a}\sqrt{b+c}}erfc\left(\frac{y}{2}\sqrt{\frac{a}{t}}-\sqrt{(b+c)t}\right)\right],$$

$$F_2(y,t,a,b,c)=\frac{e^{ct}}{2}\left[\left(t+\frac{y}{2}\sqrt{\frac{a}{b+c}}\right)e^{y\sqrt{a}\sqrt{b+c}}erfc\left(\frac{y}{2}\sqrt{\frac{a}{t}}+\sqrt{(b+c)t}\right)\right.$$
$$\left.+\left(t-\frac{y}{2}\sqrt{\frac{a}{b+c}}\right)e^{-y\sqrt{a}\sqrt{b+c}}erfc\left(\frac{y}{2}\sqrt{\frac{a}{t}}-\sqrt{(b+c)t}\right)\right]. \tag{29}$$

Solutions (23) and (26) are not valid when $P_r=1$ and $S_c=1$ which corresponds to those fluids whose viscous, thermal and concentration boundary layer thickness are of same order of magnitude. For such fluids velocity can be obtained by putting $P_r=1$ and $S_c=1$ in Equations (19) and (20), solving Equations (19) and (20) subject to the boundary conditions (21) and (22) and then inverting. In this case of solutions for velocity field are given by the following.

For uniform plate temperature:

$$F(y,\ t)=F_1(y,\ t,\ 1,\ m_3,1)+\frac{G_T}{(\phi-m_3)}\{F_1(y,\ t,\ 1,\ m_3,\ 0)-F_1(y,\ t,\ 1,\ \phi,\ 0)\}$$
$$+\frac{G_C}{(K_1-m_3)}\{F_2(y,\ t,\ 1,\ m_3,\ 0)-F_2(y,\ t,\ 1,\ K_1,\ 0)\}. \tag{30}$$

For ramped plate temperature:

$$F(y,\ t)=F_1(y,\ t,\ 1,\ m_3,\ 1)+\frac{G_T}{(\phi-m_3)}\{F_2(y,\ t,\ 1,\ m_3,\ 0)-F_2(y,\ t,\ 1,\ \phi,\ 0)$$
$$-H(t-1)\{F_2(y,\ t-1,\ 1,\ m_3,\ 0)-F_2(y,\ t-1,\ 1,\ \phi,\ 0)\}\}$$
$$+\frac{G_C}{(K_1-m_3)}\{F_2(y,\ t,\ 1,\ m_3,\ 0)-F_2(y,\ t,\ 1,\ K_1,\ 0)\}. \tag{31}$$

3.1 Skin friction

The skin friction τ_x and τ_z at the plate in the primary and secondary flow directions in case of uniform plate temperature and ramped plate temperature when $P_r\neq 1$ and $S_c\neq 1$ are given by the following.

For uniform plate temperature:

$$\tau_x+i\tau_z=F_3(t,\ 1,\ m_3,\ 1)+\frac{G_T}{X_1(P_r-1)}\{F_3(t,\ 1,\ m_3,\ 0)-F_3(t,\ P_r,\ \phi,\ 0)$$
$$-F_3(t,\ 1,\ m_3,\ -X_1)+F_3(t,\ P_r,\ \phi,\ -X_1)\}$$
$$-\frac{G_C}{X_2^2(S_c-1)}\{F_3(t,\ 1,\ m_3,\ 0)-F_3(t,\ S_c,\ K_1,\ 0)-F_3(t,\ 1,\ m_3,\ -X_2)$$
$$+F_3(t,\ S_c,\ K_1,\ -X_2)-X_2\{F_4(t,\ 1,\ m_3,\ 0)-F_4(t,\ S_c,\ K_1,\ 0)\}\}. \tag{32}$$

For ramped plate temperature:

$$\tau_x + i\tau_z = F_3(t,\ 1,\ m_3,\ 1) + \frac{G_T}{(P_r-1)}\frac{1}{X_1^2}\big[\{X_1(F_4(t,\ 1,\ m_3,\ 0) - F_4(t,\ P_r,\ \phi,\ 0))$$
$$-(F_3(t,\ 1,\ m_3,\ 0) - F_3(t,\ P_r,\ \phi,\ 0) - F_3(t,\ 1,\ m_3,\ -X_1) + F_3(t,\ P_r,\ \phi,\ -X_1))\}$$
$$-H(t-1)\{X_1(F_4(t-1,\ 1,\ m_3,\ 0) - F_4(t-1,\ P_r,\ \phi,\ 0)) - (F_3(t-1,\ 1,\ m_3,\ 0)$$
$$-F_3(t-1,\ P_r,\ \phi,\ 0) - F_3(t-1,\ 1,\ m_3,\ -X_1) + F_3(t-1,\ P_r,\ \phi,\ -X_1))\}\big]$$
$$+\frac{G_C}{(S_c-1)}\frac{1}{X_2^2}[X_2(F_4(t,\ 1,\ m_3,\ 0) - F_4(t,\ S_c,\ K_1,\ 0)) - (F_3(t,\ 1,\ m_3,\ 0)$$
$$-F_3(t,\ S_c,\ K_1,\ 0) - F_3(t,\ 1,\ m_3,\ -X_2) + F_3(\ t,\ S_c,\ K_1,\ -X_2))], \tag{33}$$

where:

$$F_3(t,a,b,c) = e^{ct}\left[\sqrt{a(b+c)}\left\{erfc\sqrt{(b+c)t} - 1\right\} - \sqrt{\frac{a}{\pi t}}\,e^{-(b+c)t}\right],$$

$$F_4(t,a,b,c) = e^{ct}\left[\left(t\sqrt{a(b+c)} + \frac{1}{2}\sqrt{\frac{a}{b+c}}\right)\left\{erfc\sqrt{(b+c)t} - 1\right\}.-\sqrt{\frac{at}{\pi}}e^{-(b+c)t}\right].$$

The skin friction τ_x and τ_z in primary and secondary flow directions in case of uniform plate temperature and ramped plate temperature when $P_r = 1$ and $S_c = 1$ are given by the following.

For uniform plate temperature:

$$\tau_x + i\tau_z = F_3(t,1,m_3,1) + \frac{G_T}{(\phi - m_3)}\{F_3(t,1,m_3,0) - F_3(t,1,\phi,0)\}$$
$$+\frac{G_C}{(K_1 - m_3)}\{F_4(t,1,m_3,0) - F_4(t,1,K_1,0)\}. \tag{34}$$

For ramped plate temperature:

$$\tau_x + i\tau_z = F_3(t,1,m_3,1) + \frac{G_T}{(\phi - m_3)}\{F_4(t,1,m_3,0) - F_4(t,1,\phi,0)$$
$$-H(t-1)\{F_4(t-1,1,m_3,0) - F_4(t-1,1,\phi,0)\}\}$$
$$+\frac{G_C}{(K_1 - m_3)}\{F_4(t,1,m_3,0) - F_4(t,1,K_1,0)\}. \tag{35}$$

3.2 Nusselt number

The Nusselt number N_u in case of uniform plate and ramped plate temperatures are given by the following.

For uniform plate temperature:

$$N_u = F_3(t,P_r,\phi,0). \tag{36}$$

For ramped plate temperature:

$$N_u = F_4(t,P_r,\phi,0) - H(t-1)F_4(t-1,P_r,\phi,0). \tag{37}$$

3.3 Sherwood number

The Sherwood number S_h is given by:

$$S_h = F_4(t, S_c, K_1, 0). \qquad (38)$$

4. Validation of the results

Singh, Joshi, Begum and Srinivasa (2016) investigated the effects of Hall current and rotation on unsteady hydromagnetic heat and mass transfers natural convection flow past an exponentially accelerated vertical plate in the presence of thermal and mass diffusions. They obtained the exact solution for fluid velocity considering both the uniform and ramped plate temperature and fluctuating concentration in the absence of ion-slip current, whereas we obtain the exact solution for fluid velocity in the presence of ion-slip current. To compare our result of skin friction at the plate in the primary flow direction with those of Singh, Joshi, Begum and Srinivasa (2016) as a special case, i.e. in the absence of ion-slip current ($\beta_i = 0$), we have computed numerical values of skin friction at the plate in the primary flow direction for our problem as well as those of Singh, Joshi, Begum and Srinivasa (2016), which are presented in Table I. It is noticed that there is good agreement between both the results.

5. Results and analysis

To examine the physical characteristic of the present physical problem, numerical computation is carried out for several sets of values of Hall current parameter (β_e), ion-slip parameter (β_i), rotation parameter (K^2), magnetic parameter (M^2), permeability parameter (k_1), thermal Grashof number (G_T), solutal Grashof number (G_C), Prandtl number (P_r), Schmidt number (S_C), heat absorption parameter (ϕ) and chemical reaction parameter (K_1). In order to analyze the salient features of the fluid flow, the numerical results for fluid velocity, temperature and species concentration are presented in graphical form in Figures 2-16, while the numerical results for skin friction at the plate, Nusselt number and Sherwood number are presented in tabular form in Tables II-IV. In the numerical computation, the boundary condition $y \to \infty$ is approximated by $y_{\max}$ which is sufficiently large for velocity, temperature and species concentration to approach their free stream value.

Figure 2 is plotted to show the influence of Hall current parameter β_e on the fluid velocity. Figure 2 shows that, in case of both the uniform and ramped plate temperature, fluid velocity of both the primary and secondary flow directions increases on increasing Hall current parameter β_e. The usual nature of Hall current is to induce fluid velocity in the secondary flow direction. Our result agrees with it. Figure 3 exhibits the effects of ion-slip parameter β_i on the velocity profiles. In both the uniform and ramped plate temperature cases, the primary fluid velocity increases whereas the secondary fluid velocity decreases

	Uniform plate temperature			Ramped plate temperature		
	K^2					
β_e	1	3	5	1	3	5
Present numerical values						
0.25	4.5803	4.8474	5.2094	5.0774	5.3084	5.6271
0.75	4.0179	4.4495	4.9254	4.5351	4.9069	5.3286
1.25	3.4007	3.9574	4.5207	3.9535	4.4277	4.9257
Numerical values by Singh, Joshi, Begum and Srinivasa (2016)						
0.25	4.5803	4.8474	5.2094	5.0774	5.3084	5.6271
0.75	4.0179	4.4495	4.9254	4.5351	4.9069	5.3286
1.25	3.4007	3.9574	4.5207	3.9535	4.4277	4.9257

Table I. Skin friction at the plate in the primary flow direction ($-\tau_x$) when $M^2 = 9$, $k_1 = 0.3$, $G_T = 4$, $G_C = 5$, $P_r = 0.71$, $S_c = 0.22$, $\phi = 1$, $K_1 = 0.2$ and $t = 0.5$

with increase in ion-slip parameter. Figure 4 is plotted to examine the role of rotation parameter K^2 on velocity profiles. In case of both the uniform and ramped plate temperature, Coriolis force tends to reduce fluid velocity in the primary flow direction whereas it has reverse nature on the fluid velocity in the secondary flow direction. Similar to Hall current the usual nature of Coriolis force is to generate fluid flow in the secondary flow direction. Our results comply with it. The variation of fluid velocity for various values of magnetic parameter is rendered in Figure 5. Figure 5 illustrates that, in case of both the uniform and ramped plate temperature, the fluid velocity in the primary flow direction

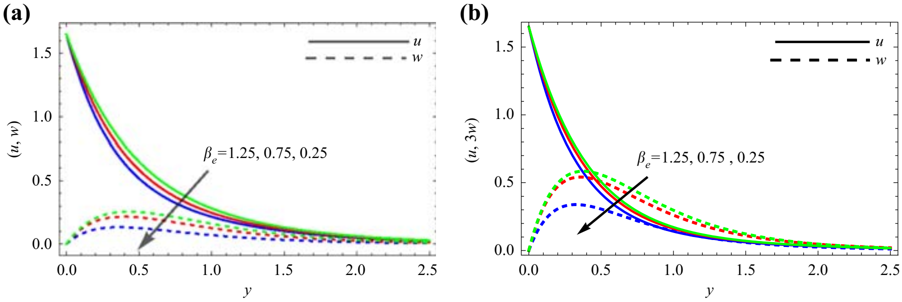

Figure 2.
Velocity distribution when $\beta_i = 0.5$, $K^2 = 1$, $M^2 = 9$, $k_1 = 0.3$, $G_T = 4$, $G_C = 5$, $P_r = 0.71$, $S_c = 0.22$, $\phi = 1$, $K_1 = 0.2$ and $t = 0.5$

Notes: (a) Uniform plate temperature; (b) ramped plate temperature

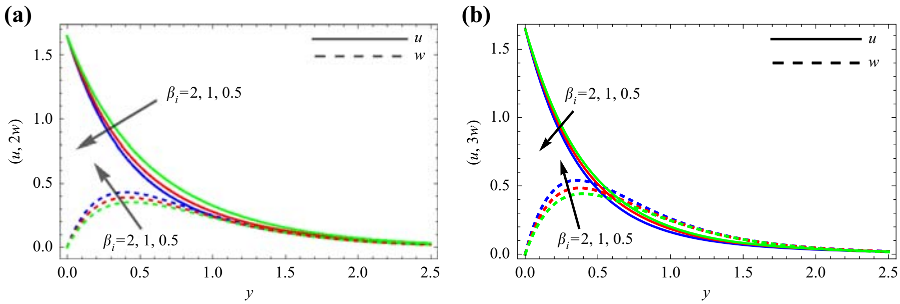

Figure 3.
Velocity distribution when $\beta_e = 0.75$, $K^2 = 1$, $M^2 = 9$, $k_1 = 0.3$, $G_T = 4$, $G_C = 5$, $P_r = 0.71$, $S_c = 0.22$, $\phi = 1$, $K_1 = 0.2$ and $t = 0.5$

Notes: (a) Uniform plate temperature; (b) ramped plate temperature

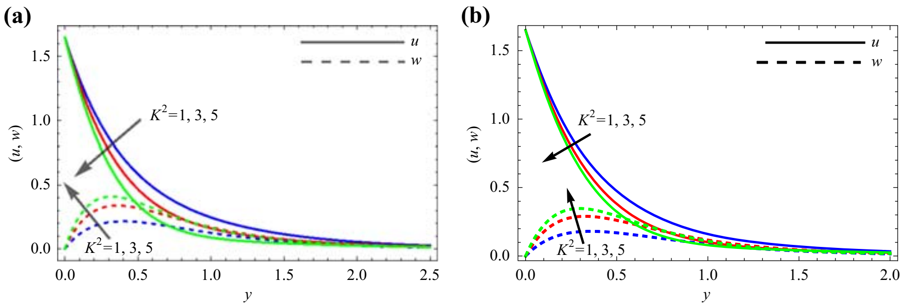

Figure 4.
Velocity distribution when $\beta_e = 0.75$, $\beta_i = 0.5$, $M^2 = 9$, $k_1 = 0.3$, $G_T = 4$, $G_C = 5$, $P_r = 0.71$, $S_c = 0.22$, $\phi = 1$, $K_1 = 0.2$ and $t = 0.5$

Notes: (a) Uniform plate temperature; (b) ramped plate temperature decreases with increase in magnetic parameter. The fluid velocity in the secondary flow direction increases in the vicinity of the plate while it decreases in the boundary layer region away from the plate with increase in magnetic parameter. This is due to the fact that applied magnetic field produces a drag force in the form of Lorentz force which is generated due to the motion of charge particles, which decrease the magnitude of velocity. Figure 6 demonstrate that, in case of both uniform and ramped plate temperature, fluid velocity in both the primary and secondary flow directions increases on increasing permeability parameter k_1, which implies that permeability tends to enhance fluid velocity in both the primary and secondary flow directions, i.e. Darcian drag force tends to reduce the fluid

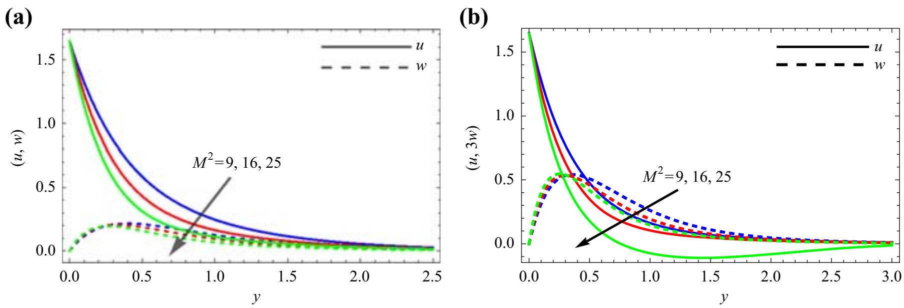

Notes: (a) Uniform plate temperature; (b) ramped plate temperature

Figure 5. Velocity distribution when $\beta_e = 0.75$, $\beta_i = 0.5$, $K^2 = 1$, $k_1 = 0.3$, $G_T = 4$, $G_C = 5$, $P_r = 0.71$, $S_c = 0.22$, $\phi = 1$, $K_1 = 0.2$ and $t = 0.5$

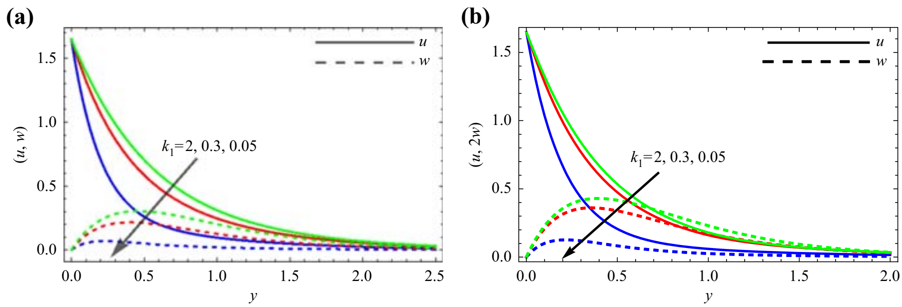

Notes: (a) Uniform plate temperature; (b) ramped plate temperature

Figure 6. Velocity distribution when $\beta_e = 0.75$, $\beta_i = 0.5$, $K^2 = 1$, $M^2 = 9$, $G_T = 4$, $G_C = 5$, $P_r = 0.71$, $S_c = 0.22$, $\phi = 1$, $K_1 = 0.2$ and $t = 0.5$

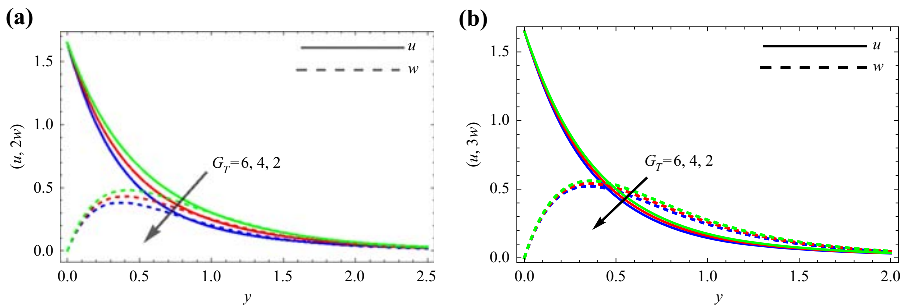

Notes: (a) Uniform plate temperature; (b) ramped plate temperature

Figure 7. Velocity distribution when $\beta_e = 0.75$, $\beta_i = 0.5$, $K^2 = 1$, $M^2 = 9$, $k_1 = 0.3$, $G_C = 5$, $P_r = 0.71$, $S_c = 0.22$, $\phi = 1$, $K_1 = 0.2$ and $t = 0.5$

velocity in both the primary and secondary flow directions (when permeability is weak, Darcian drag force is strong). The effect of thermal Grashof number G_T and solutal Grashof number G_C on velocity profiles is visually represented in Figures 7 and 8. These figures exhibit that, in case of both the uniform and ramped plate temperature, the fluid velocity in both the primary and secondary flow directions increases on increasing both the thermal and solutal Grashof numbers. This concludes that both the thermal and concentration buoyancy forces tend to enhance the fluid velocity in both the primary and secondary flow directions. Figures 9-12, respectively, illustrate the effects of Prandtl number P_r, Schmidt number S_c, heat absorption parameter ϕ and chemical reaction parameter K_1 on the fluid

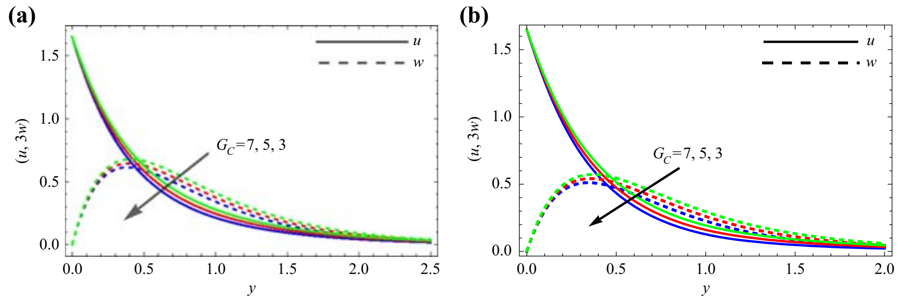

Figure 8. Velocity distribution when $\beta_e = 0.75$, $\beta_i = 0.5$, $K^2 = 1$, $M^2 = 9$, $k_1 = 0.3$, $G_T = 4$, $P_r = 0.71$, $S_c = 0.22$, $\phi = 1$, $K_1 = 0.2$ and $t = 0.5$

Notes: (a) Uniform plate temperature; (b) ramped plate temperature

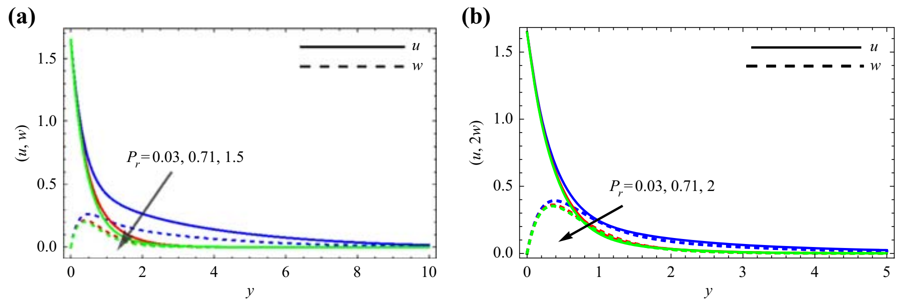

Figure 9. Velocity distribution when $\beta_e = 0.75$, $\beta_i = 0.5$, $K^2 = 1$, $M^2 = 9$, $k_1 = 0.3$, $G_T = 4$, $G_C = 5$, $S_c = 0.22$, $\phi = 1$, $K_1 = 0.2$ and $t = 0.5$

Notes: (a) Uniform plate temperature; (b) ramped plate temperature

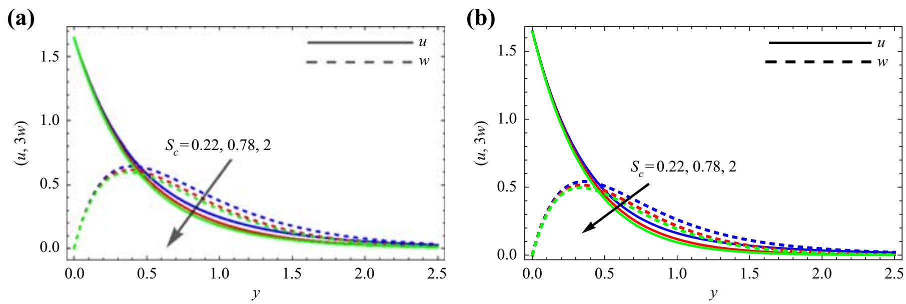

Figure 10. Velocity distribution when $\beta_e = 0.75$, $\beta_i = 0.5$, $K^2 = 1$, $M^2 = 9$, $k_1 = 0.3$, $G_T = 4$, $G_C = 5$, $P_r = 0.71$, $\phi = 1$, $K_1 = 0.2$ and $t = 0.5$

Notes: (a) Uniform plate temperature; (b) ramped plate temperature velocity. In case of both the uniform and ramped plate temperature, velocity profiles decrease for increasing values of Prandtl number P_r, Schmidt number S_c, heat absorption parameter ϕ and chemical reaction parameter K_1. Prandtl number and Schmidt number measure the relative strength of viscosity to the thermal diffusivity (thermal diffusion) and chemical molecular diffusivity (mass diffusion), respectively. Since there is an inverse

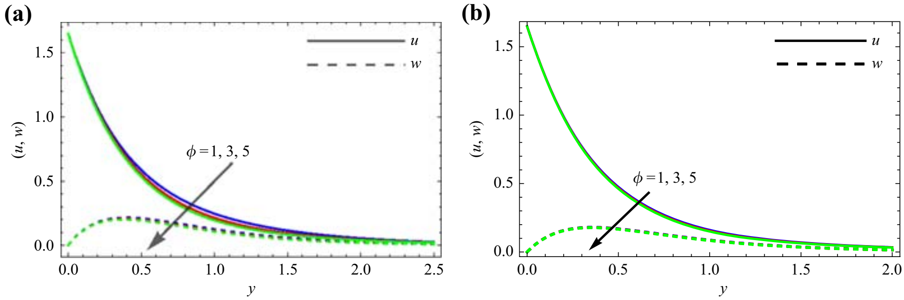

Notes: (a) Uniform plate temperature; (b) ramped plate temperature

Figure 11. Velocity distribution when $\beta_e = 0.75$, $\beta_i = 0.5$, $K^2 = 1$, $M^2 = 9$, $k_1 = 0.3$, $G_T = 4$, $G_C = 5$, $P_r = 0.71$, $S_C = 0.22$, $K_1 = 0.2$ and $t = 0.5$

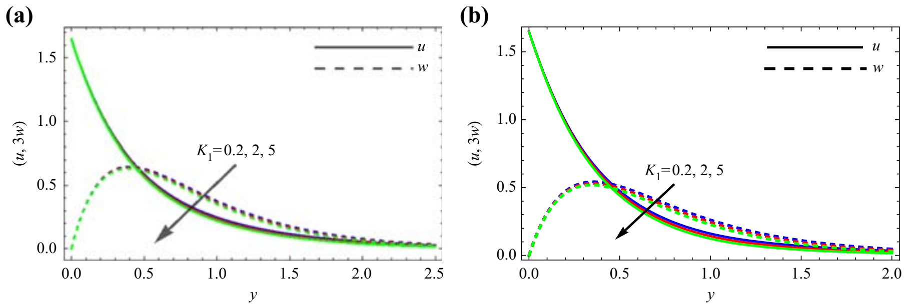

Notes: (a) Uniform plate temperature; (b) ramped plate temperature

Figure 12. Velocity distribution when $\beta_e = 0.75$, $\beta_i = 0.5$, $K^2 = 1$, $M^2 = 9$, $k_1 = 0.3$, $G_T = 4$, $G_C = 5$, $P_r = 0.71$, $S_C = 0.22$, $\phi = 1$ and $t = 0.5$

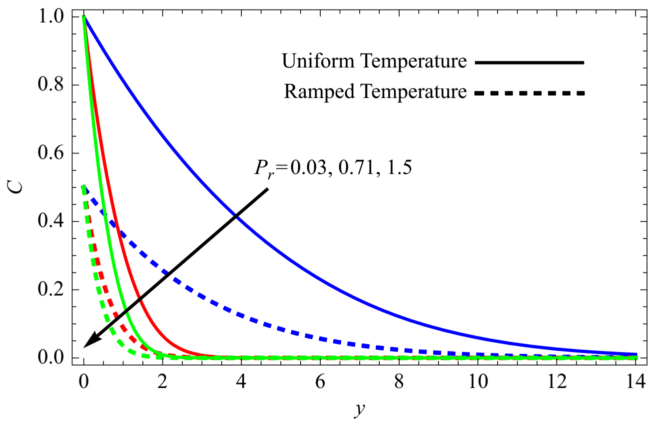

Figure 13. Temperature distribution when $\phi = 1$

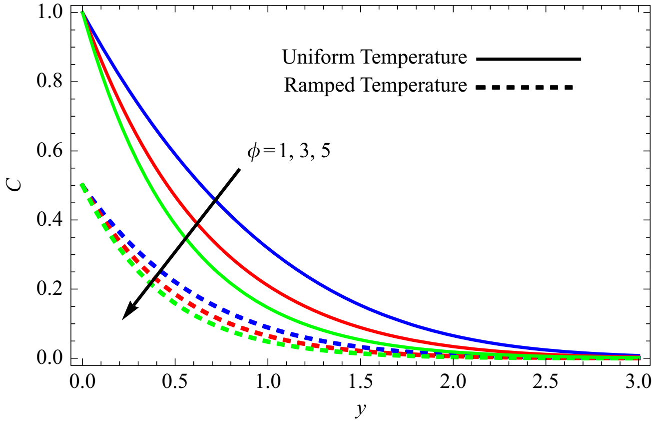

Figure 14.
Temperature distribution when $P_r = 0.71$

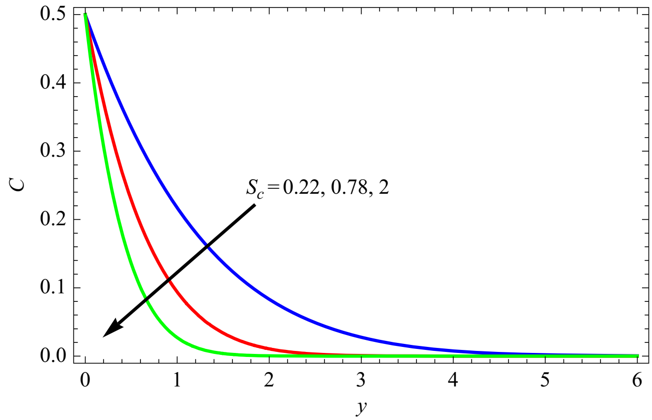

Figure 15.
Concentration distribution when $K_1 = 0.2$

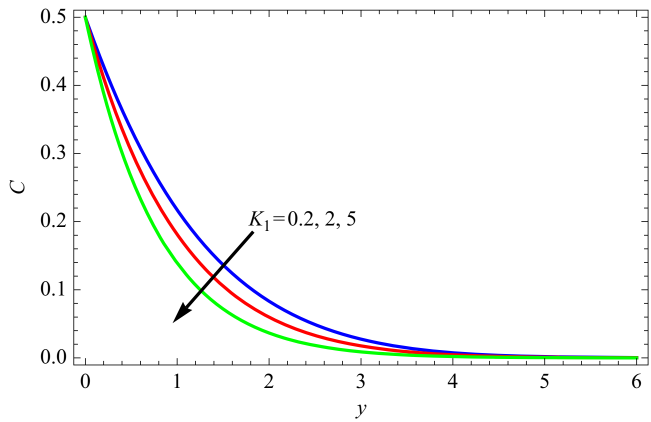

Figure 16.
Concentration distribution when $S_c = 0.22$

Table II. Skin friction at the plate in the primary and secondary flow directions

β_e	β_i	K^2	M^2	k_1	G_T	G_C	P_r	S_c	ϕ	K_1	Uniform plate temperature $-\tau_x$	Uniform plate temperature τ_z	Ramped plate temperature $-\tau_x$	Ramped plate temperature τ_z
0.75	*0.5*	*1*	*9*	*0.3*	*4*	*5*	*0.71*	*0.22*	*1*	*0.2*	3.6749	1.4997	4.2267	1.3838
0.25	0.5	1	9	0.3	4	5	0.71	0.22	1	0.2	4.3349	1.0304	4.8491	0.9606
1.25	0.5	1	9	0.3	4	5	0.71	0.22	1	0.2	3.1883	1.6260	3.7754	1.4871
0.75	*1*	1	9	0.3	4	5	0.71	0.22	1	0.2	3.3873	1.2865	3.9666	1.1806
0.75	*2*	1	9	0.3	4	5	0.71	0.22	1	0.2	2.9733	1.0801	3.5920	0.9832
0.75	0.5	*3*	9	0.3	4	5	0.71	0.22	1	0.2	4.0891	2.5744	4.5864	2.3985
0.75	0.5	*5*	9	0.3	4	5	0.71	0.22	1	0.2	4.5960	3.4497	5.0126	3.2492
0.75	0.5	1	*16*	0.3	4	5	0.71	0.22	1	0.2	4.8708	1.7591	5.3382	1.6544
0.75	0.5	1	*25*	0.3	4	5	0.71	0.22	1	0.2	6.1226	2.0302	6.5223	1.9375
0.75	0.5	1	9	*0.05*	4	5	0.71	0.22	1	0.2	7.3835	0.8446	7.7479	0.8134
0.75	0.5	1	9	*2*	4	5	0.71	0.22	1	0.2	2.7804	1.8013	3.3977	1.6344
0.75	0.5	1	9	0.3	*2*	5	0.71	0.22	1	0.2	4.1461	1.4165	4.4220	1.3585
0.75	0.5	1	9	0.3	*6*	5	0.71	0.22	1	0.2	3.2037	1.5830	4.0135	1.4091
0.75	0.5	1	9	0.3	4	*3*	0.71	0.22	1	0.2	3.9074	1.4631	4.4593	1.3472
0.75	0.5	1	9	0.3	4	*7*	0.71	0.22	1	0.2	3.4423	1.5363	3.9942	1.4204
0.75	0.5	1	9	0.3	4	5	*0.03*	0.22	1	0.2	3.4397	1.6115	4.0920	1.4294
0.75	0.5	1	9	0.3	4	5	*1.5*	0.22	1	0.2	3.7770	1.4616	4.2776	1.3708
0.75	0.5	1	9	0.3	4	5	0.71	*0.78*	1	0.2	3.7615	1.4726	4.3133	1.3567
0.75	0.5	1	9	0.3	4	5	0.71	*2*	1	0.2	3.8421	1.4523	4.3940	1.3363
0.75	0.5	1	9	0.3	4	5	0.71	0.22	*3*	0.2	3.7605	1.4779	4.2502	1.3785
0.75	0.5	1	9	0.3	4	5	0.71	0.22	*5*	0.2	3.8227	1.4570	4.2691	1.3744
0.75	0.5	1	9	0.3	4	5	0.71	0.22	1	*2*	3.6978	1.4935	4.2497	1.3775
0.75	0.5	1	9	0.3	4	5	0.71	0.22	1	*5*	3.7279	1.4853	4.2798	1.3694

relation between Prandtl number and Schmidt number to the thermal diffusivity and chemical molecular diffusivity, respectively. This implies that both the thermal and mass diffusions tend to enhance fluid velocity in both the primary and secondary flow directions, whereas heat absorption and chemical reaction have reverse effects on these which agrees with the results of Singh, Joshi, Begum and Srinivasa (2016), Seth and Sarkar (2015) and Hussain *et al.* (2017).

Influences of thermal diffusion and heat absorption on fluid temperature are demonstrated in Figures 13 and 14, respectively. Figures 13 and 14 describe that, in case of both the uniform and ramped plate temperature, fluid temperature decreases on increasing Prandtl number P_r and heat absorption parameter ϕ. This indicates that thermal diffusion tends to enhance fluid temperature whereas heat absorption has reverse effect on it. The effects of mass diffusion and chemical reaction on species concentration are displayed in Figures 15 and 16, respectively. Figures 15 and 16 illustrate that species concentration decreases on increasing Schmidt number S_c and chemical reaction parameter K_1 which concludes that mass diffusion tends to enhance species concentration whereas chemical reaction has reverse effect on it.

The skin friction at the plate is demonstrated in Table II whereas the rate of heat and mass transfers at the plate in terms of Nusselt and Sherwood numbers is presented in Tables III and IV. It is noticed from Table I that, for both the uniform and ramped temperature cases, Hall current, ion-slip current, thermal and concentration buoyancy forces, thermal diffusion and mass diffusion tend to reduce the skin friction at the plate in the primary flow direction, while Coriolis force, applied magnetic field, Darcian drag force, heat absorption and chemical reaction have reverse tendency on it. In both the uniform and ramped temperature cases, skin friction at the plate in the secondary flow direction is enhanced by Hall current, Coriolis force, applied magnetic field, thermal and concentration buoyancy forces, thermal diffusion and mass diffusion, while it is reduced by ion-slip current, Darcian drag force, heat absorption and chemical reaction. Table III displays that thermal diffusion reduces rate of heat transfer at the plate while heat absorption enhances it in case of both the uniform and ramped plate temperature. Table IV shows that the rate of mass transfer at the plate is reduced by mass diffusion while it is enhanced by chemical reaction.

Table III.
Nusselt number

P_r	ϕ	Uniform plate temperature $-Nu$	Ramped plate temperature $-Nu$
0.71	*1*	0.9830	0.7719
0.03	1	0.2020	0.1602
1.5	1	1.4288	1.1325
0.71	*3*	1.4880	0.9670
0.71	*5*	1.8916	1.1294

Table IV.
Sherwood number

S_c	K_1	$-Sh$
0.22	*0.2*	0.3870
0.78	0.2	0.7880
2	0.2	1.6756
0.22	*2*	0.4880
0.22	*5*	0.6287

6. Conclusions

A mathematical analysis has been presented for unsteady hydromagnetic heat and mass transfer natural convection flow past an exponentially accelerated vertical plate in a uniform porous medium taking Hall current and ion-slip into account with variable species concentration and uniform/variable plate temperature. Following conclusions are made from this analysis:

- Hall current tends to enhance fluid velocity in the primary flow direction whereas Coriolis force and magnetic field have reverse effect on it. Both the Hall current and Coriolis force tend to enhance fluid velocity in the secondary flow direction.
- Ion-slip current enhances fluid flow in the primary flow direction whereas it has reverse effect on the fluid flow in the secondary flow direction.
- Magnetic field has tendency to enhance fluid velocity in the secondary flow direction in the vicinity of the plate whereas it has reverse effect in the boundary layer region away from the plate.
- Thermal and concentration buoyancy forces tend to enhance fluid velocity in both the primary and secondary flow directions whereas Darcian drag force, thermal and mass diffusions have reverse effect on these.
- Thermal diffusion tends to enhance fluid temperature whereas heat absorption has reverse effect on it.
- Mass diffusion tends to enhance species concentration whereas chemical reaction has reverse effect on it.
- Hall current, ion-slip current, thermal and concentration buoyancy forces, thermal diffusion and mass diffusion tend to reduce the skin friction at the plate in the primary flow direction while Coriolis force, applied magnetic field, Darcian drag force, heat absorption and chemical reaction have reverse tendency on it.
- Hall current, Coriolis force, applied magnetic field, thermal and concentration buoyancy forces, thermal diffusion and mass diffusion enhance skin friction at the plate in the secondary flow direction while ion-slip current, Darcian drag force, heat absorption and chemical reaction reduce it.
- Thermal diffusion reduces rate of heat transfer at the plate while heat absorption enhances it.
- The rate of mass transfer at the plate is reduced by mass diffusion while it is enhanced by chemical reaction.

References

Cramer, K.R. and Pai, S.I. (1973), *Magnetofluid-Dynamics for Engineers and Applied Physicists*, McGraw-Hill, New York, NY.

Das, K., Jana, S. and Kundu, P.K. (2014), "Unsteady MHD free convection flow near a moving vertical plate with ramped wall temperature", *International Journal of Fluid Mechanics Research*, Vol. 41 No. 1, pp. 71-90.

Foisal, A.A. and Alam, M.M. (2016), "Unsteady free convection fluid flow over an inclined plate in the presence of a magnetic field with thermally stratified high porosity medium", *Journal of Applied Fluid Mechanics*, Vol. 9 No. 3, pp. 1467-1475.

Gireesha, B.J., Mahanthesh, B., Gorla, R.S.R. and Manjunatha, P.T. (2016), "Thermal radiation and Hall effects on boundary layer flow past a non-isothermal stretching surface embedded in porous medium with non-uniform heat source/sink and fluid particle suspension", *Heat and Mass Transfer*, Vol. 52 No. 4, pp. 897-911.

Greenspan, H.P. and Howard, L.N. (1963), "On a time-dependent motion of a rotating fluid", *Journal of Fluid Mechanics*, Vol. 17 No. 3, pp. 385-404.

Hayat, T., Shafique, M., Tanveer, A. and Alsaedi, A. (2016), "Hall and ion slip effects on peristaltic flow of Jeffrey nanofluid with Joule heating", *Journal of Magnetism and Magnetic Materials*, Vol. 407 No. 1, pp. 1-59.

Hossain, M.A., Mondal, R.K., Ahmed, R. and Ahmmed, S.F. (2015), "A numerical study on unsteady natural convection flow with temperature dependent viscosity past an isothermal vertical cylinder", *Journal of Pure Applied and Industrial Physics*, Vol. 5 No. 5, pp. 125-135.

Hussain, S.M., Jain, J., Seth, G.S. and Rashidi, M.M. (2017), "Free convective heat transfer with hall effects, heat absorption and chemical reaction over an accelerated moving plate in a rotating system", *Journal of Magnetism and Magnetic Materials*, Vol. 422 No. 15, pp. 112-123.

Krishnamurthy, M.R., Prasannakumara, B.C., Gireesha, B.J. and Gorla, R.S.R. (2016), "Effect of chemical reaction on MHD boundary layer flow and melting heat transfer of Williamson nanofluid in porous medium", *Engineering Science and Technology: An International Journal*, Vol. 19 No. 1, pp. 53-61.

Lin, W. and Armfield, S.W. (2017), "Scalings for unsteady natural convection boundary layers on a vertical plate at time-dependent temperature", *International Journal of Thermal Sciences*, Vol. 111, pp. 78-99.

Meyer, R.C. (1958), "On reducing aerodynamic heat-transfer rates by magnetohydrodynamic technique", *Journal of the Aerospace Sciences*, Vol. 25 No. 9, pp. 561-566.

Mohamad, A.Q., Khan, I., Shafie, S., Isa, Z.M. and Ismail, Z. (2017), "Non-coaxial rotating flow of viscous fluid with heat, and mass transfer", *Neural Computing and Applications*, pp. 1-11, doi: 10.1007/s00521-017-2854-6.

Mustafa, M., Wasim, M., Hayat, T. and Alsaedi, A. (2017), "A revised model to study the rotating flow of nanofluid over an exponentially deforming sheet: numerical solutions", *Journal of Molecular Liquids*, Vol. 225, pp. 320-327.

Nazar, R., Amin, N. and Pop, I. (2004), "Unsteady boundary layer flow due to a stretching surface in a rotating fluid", *Mechanics Research Communications*, Vol. 31 No. 1, pp. 121-128.

Ram, P.C. (1995), "Effects of hall and ion-slip currents on free convective heat generating flow in a rotating fluid", *International Journal of Energy Research*, Vol. 19 No. 5, pp. 371-376.

Sarma, D. and Pandit, K.K. (2016), "Effects of Hall current, rotation and Soret effects on MHD free convection heat and mass transfer flow past an accelerated vertical plate through a porous medium", *Ain Shams Engineering Journal*, doi: 10.1016/j.asej.2016.03.005.

Seth, G.S. and Sarkar, S. (2015), "Hydromagnetic natural convection flow with induced magnetic field and nth order chemical reaction of a heat absorbing fluid past an impulsively moving vertical plate with ramped temperature", *Bulgarian Chemical Communications*, Vol. 47 No. 1, pp. 66-79.

Singh, J.K., Begum, S.G. and Joshi, N. (2016), "Effects of hall current and ion-slip on unsteady hydromagnetic generalised Couette flow in a rotating Darcian channel", *Journal of Mathematical Modelling*, Vol. 3 No. 2, pp. 145-167.

Singh, J.K., Joshi, N., Begum, S.G. and Srinivasa, C.T. (2016), "Unsteady hydromagnetic heat and mass transfer natural convection flow past on exponentially accelerated vertical plate with Hall current and rotation in the presence of thermal and mass diffusion", *Frontiers in Heat and Mass Transfer*, Vol. 7 No. 24, pp. 1-12.

Srinivasacharya, D. and Shafeeurrahaman, M. (2017), "Mixed convection flow of nanofluid in a vertical channel with hall and ion-slip effects", *Frontiers in Heat and Mass Transfer*, Vol. 11, pp. 1-8.

Sutton, G. and Sherman, A. (1965), *Engineering Magnetohydrodynamics*, McGraw-Hill, New York, NY.

Tkachenko, O.A., Timchenko, V., Giroux-Julien, S., Ménézo, C., Yeoh, G.H., Reizes, J.A., Sanvicente, E. and Fossa, M. (2016), "Numerical and experimental investigation of unsteady natural convection in a non-uniformly heated vertical open-ended channel", *International Journal of Thermal Sciences*, Vol. 99, pp. 9-25.

Zargartalebi, H., Ghalambaz, M., Khanafer, K. and Pop, I. (2017), "Unsteady conjugate natural convection in a porous cavity boarded by two vertical finite thickness walls", *International Communications in Heat and Mass Transfer*, Vol. 81, pp. 218-228.

Corresponding author
Srinivasa C.T. can be contacted at: srinivasact@rediffmail.com